PAPER

Weight dependence of local exchange–correlation functionals in ensemble density-functional theory: double excitations in two-electron systems

Clotilde Marut, [a] Bruno Senjean, [bc] Emmanuel Fromager [d] and Pierre-François Loos *[a]

Gross–Oliveira–Kohn (GOK) ensemble density-functional theory (GOK-DFT) is a time-independent extension of density-functional theory (DFT) which allows the computation of excited-state energies *via* the derivatives of the ensemble energy with respect to the ensemble weights. Contrary to the time-dependent version of DFT (TD-DFT), double excitations can be easily computed within GOK-DFT. However, to take full advantage of this formalism, one must have access to a weight-dependent exchange–correlation functional in order to model the infamous ensemble derivative contribution to the excitation energies. In the present article, we discuss the construction of first-rung (*i.e.*, local) weight-dependent exchange–correlation density-functional approximations for two-electron atomic and molecular systems (He and H_2) specifically designed for the computation of double excitations within GOK-DFT. In the spirit of optimally-tuned range-separated hybrid functionals, a two-step system-dependent procedure is proposed to obtain accurate energies associated with double excitations.

I.   Introduction

Time-dependent density-functional theory (TD-DFT) has been the dominant force in the calculation of excitation energies of molecular systems in the last two decades.[1–3] At a moderate computational cost (at least compared to the other excited-state *ab initio* methods), TD-DFT can provide accurate transition energies for low-lying excited states of organic molecules (see, for example, ref. 4 and references therein). Importantly, within the widely-used adiabatic approximation,

[a]Laboratoire de Chimie et Physique Quantiques, Université de Toulouse, CNRS, UPS, France. E-mail: loos@irsamc.ups-tlse.fr

[b]Instituut-Lorentz, Universiteit Leiden, P. O. Box 9506, 2300 RA Leiden, The Netherlands

[c]Division of Theoretical Chemistry, Vrije Universiteit Amsterdam, De Boelelaan 1083, 1081 HV Amsterdam, The Netherlands

[d]Laboratoire de Chimie Quantique, Institut de Chimie, CNRS, Université de Strasbourg, Strasbourg, France

setting up a TD-DFT calculation for a given system is an almost pain-free process from a user perspective, as the only (yet essential) input variable is the choice of the ground-state exchange–correlation (xc) functional.

Similar to density-functional theory (DFT),[5–7] TD-DFT is an in-principle exact theory in which formal foundations rely on the Runge–Gross theorem.[8] The Kohn–Sham (KS) formulation of TD-DFT transfers the complexity of the many-body problem to the xc functional thanks to judicious mapping between a time-dependent non-interacting reference system and its interacting analog which both have exactly the same one-electron density.

However, TD-DFT is far from being perfect as, in practice, drastic approximations must be made. First, within the commonly used linear-response regime, the electronic spectrum relies on the (unperturbed) pure-ground-state KS picture,[1,8,9] which may not be adequate in certain situations (such as strong correlation). Second, the time dependence of the functional is usually treated at the local approximation level within the standard adiabatic approximation. In other words, memory effects are absent from the xc functional which is assumed to be local in time (the xc energy is in fact an xc action, not an energy functional).[10] Third and more importantly in the present context, a major issue of TD-DFT actually originates directly from the choice of the (ground-state) xc functional, and more specifically, the possible (not to say likely) substantial variations in the quality of the excitation energies for two different choices of xc functionals.

Because of its popularity, approximate TD-DFT has been studied extensively, and some researchers have quickly unveiled various theoretical and practical deficiencies. For example, TD-DFT has problems with charge-transfer[11–15] and Rydberg[16–20] excited states (the excitation energies are usually drastically underestimated) due to the wrong asymptotic behaviour of the semi-local xc functional. The development of range-separated hybrids provides an effective solution to this problem.[21,22] From a practical point of view, the TD-DFT xc kernel is usually considered as static instead of being frequency dependent. One key consequence of this so-called adiabatic approximation (based on the assumption that the density varies slowly with time) is that double excitations are completely absent from the TD-DFT spectra.[17,23,24] Although these double excitations are usually experimentally dark (which means that they usually cannot be observed in photo-absorption spectroscopy), these states play, indirectly, a key role in many photochemistry mechanisms.[25] They are, moreover, a real challenge for high-level computational methods.[26–28]

One possible solution to access double excitations within TD-DFT is provided by spin-flip TD-DFT which describes double excitations as single excitations from the lowest triplet state.[29–34] However, spin contamination might be an issue.[29] Note that a simple remedy based on a mixed reference reduced density matrix has been recently introduced by Lee *et al.*[35] In order to go beyond the adiabatic approximation, a dressed TD-DFT approach has been proposed by Maitra and coworkers[36,37] (see also ref. 24 and 38–41). In this approach the xc kernel is made frequency dependent, which allows to treat doubly-excited states.[27,42,43]

Maybe surprisingly, another possible way of accessing double excitations is to resort to a time-independent formalism.[44–46] With a computational cost similar to traditional KS-DFT, DFT for ensembles (eDFT)[47–50] is a viable alternative that follows such a strategy and is currently under active development.[44–46,51–81] Assuming monotonically decreasing weights for increasing energy states, eDFT for excited states has the undeniable advantage of being based on a rigorous

variational principle for ground and excited states, the so-called Gross–Oliveria–Kohn (GOK) variational principle.[48] In short, GOK-DFT (*i.e.*, eDFT for neutral excitations) is the density-based analog of state-averaged wave function methods, and excitation energies can then be easily extracted from the total ensemble energy.[46] Although the formal foundations of GOK-DFT were set three decades ago,[48–50] its practical developments have been rather slow. We believe that it is partly due to the lack of accurate approximations for GOK-DFT. In particular, to the best of our knowledge, although several attempts have been made,[82,83] an explicitly weight-dependent density-functional approximation for ensembles (eDFA) has never been developed for atoms and molecules from first principles. The present contribution paves the way towards this goal.

The local-density approximation (LDA), as we know it, is based on the uniform electron gas (UEG) also known as jellium, a hypothetical infinite substance where an infinite number of electrons "bathe" in a (uniform) positively-charged jelly.[84] Although the Hohenberg–Kohn theorems[5] are here to provide firm theoretical grounds to DFT, modern KS-DFT rests largely on the presumed similarity between this hypothetical UEG and the electronic behaviour in a real system.[6] However, Loos and Gill have recently shown that there exists other UEGs which contain finite numbers of electrons (more like in a molecule),[85,86] and that they can be exploited to construct ground-state functionals as shown in ref. 87–89, where the authors proposed generalised LDA exchange and correlation functionals.

Electrons restricted to remain on the surface of a $\mathscr{D}$-sphere (where $\mathscr{D}$ is the dimensionality of the surface of the sphere) are an example of finite UEGs (FUEGs).[85] Very recently,[90] two of the present authors took advantage of these FUEGs to construct a local, weight-dependent correlation functional specifically designed for one-dimensional many-electron systems. Unlike any standard functional, this first-rung functional automatically incorporates ensemble derivative contributions thanks to its natural weight dependence,[91,92] and has shown to deliver accurate excitation energies for both single and double excitations. In order to extend this methodology to more realistic (atomic and molecular) systems, we combine here these FUEGs with the usual infinite UEG (IUEG) to construct a weight-dependent LDA correlation functional for ensembles, which is specifically designed to compute double excitations within GOK-DFT.

This paper is organised as follows. In Section II, the theory behind GOK-DFT is briefly presented. Section III provides the computational details. The results of our calculations for two-electron systems are reported and discussed in Section IV. Finally, we draw our conclusions in Section V. Unless otherwise stated, atomic units are used throughout.

II.   Theory

Let us consider a GOK ensemble of M electronic states with individual energies $E^{(0)} \leq \ldots \leq E^{(M-1)}$, and (normalised) monotonically decreasing weights $\boldsymbol{w} \equiv (w_1, \ldots, w_{M-1})$, *i.e.*, $w_0 = 1 - \sum_{I=1}^{M-1} w_I$, and $w_0 \geq \ldots \geq w_{M-1}$. The corresponding ensemble energy

$$E^{\boldsymbol{w}} = \sum_{I=0}^{M-1} w_I E^{(I)} \tag{1}$$

can be obtained from the GOK variational principle as follows[48]

$$E^w = \min_{\widehat{\Gamma}^w} \text{Tr}\left[\widehat{\Gamma}^w \hat{H}\right], \tag{2}$$

where $\hat{H} = \hat{T} + \hat{W}_{ee} + \hat{V}_{ne}$ contains the kinetic, electron–electron and nuclei–electron interaction potential operators, respectively, Tr denotes the trace, and $\hat{\Gamma}^w$ is a trial density matrix operator of the form

$$\widehat{\Gamma}^w = \sum_{I=0}^{M-1} w_I \left|\bar{\Psi}^{(I)}\right\rangle\left\langle\bar{\Psi}^{(I)}\right|, \tag{3}$$

where $\{\bar{\Psi}^{(I)}\}_{0 \leq I \leq M-1}$ is a set of M orthonormal trial wave functions. The lower boundary of eqn (2) is reached when the set of wave functions correspond to the exact eigenstates of $\hat{H}$, i.e., $\{\bar{\Psi}^{(I)}\}_{0 \leq I \leq M-1} = \{\Psi^{(I)}\}_{0 \leq I \leq M-1}$. Multiplet degeneracies can be easily handled by assigning the same weight to the degenerate states.[49] One of the key features of the GOK ensemble is that excitation energies can be extracted from the ensemble energy *via* differentiation with respect to the individual excited-state weights w_I ($I > 0$):

$$\frac{\partial E^w}{\partial w_I} = E^{(I)} - E^{(0)} = \Omega^{(I)}. \tag{4}$$

Turning to GOK-DFT, the extension of the Hohenberg–Kohn theorem to ensembles allows us to rewrite the exact variational expression for the ensemble energy as[49]

$$E^w = \min_n\left\{F^w[n] + \int v_{ne}(\boldsymbol{r})n(\boldsymbol{r})\mathrm{d}\boldsymbol{r}\right\}, \tag{5}$$

where $v_{ne}(\boldsymbol{r})$ is the external potential and $F^w[n]$ is the universal ensemble functional (the weight-dependent analog of the Hohenberg–Kohn universal functional for ensembles). In the KS formulation,[49] this functional can be decomposed as

$$F^w[n] = \text{Tr}\{\hat{\gamma}^w[n]\hat{T}\} + E_H[n] + E^w_{xc}[n], \tag{6}$$

where $\text{Tr}\{\hat{\gamma}^w[n]\hat{T}\} = T_s^w[n]$ is the noninteracting ensemble kinetic energy functional,

$$\widehat{\gamma}^w[n] = \sum_{I=0}^{M-1} w_I \left|\Phi_I^w[n]\right\rangle\left\langle\Phi_I^w[n]\right| \tag{7}$$

is the density-functional KS density matrix operator, and $\{\Phi_I^w[n]\}_{0 \leq I \leq M-1}$ are single-determinant wave functions (or configuration state functions[60]). Their dependence on the density is determined from the ensemble density constraint

$$\sum_{I=0}^{M-1} w_I n_{\Phi_I^w[n]}(\boldsymbol{r}) = n(\boldsymbol{r}). \tag{8}$$

Note that the original decomposition[49] shown in eqn (6), where the conventional (weight-independent) Hartree functional

$$E_H[n] = \frac{1}{2} \iint \frac{n(r)n(r')}{r - r'} \mathrm{d}r\mathrm{d}r' \tag{9}$$

is separated from the (weight-dependent) exchange–correlation (xc) functional, is formally exact. In practice, the use of such a decomposition might be problematic as inserting an ensemble density into $E_H[n]$ causes the infamous ghost-interaction error.[51,60,68,69,74] The latter should in principle be removed by the exchange component of the ensemble xc functional $E_{xc}^w[n] \equiv E_x^w[n] + E_c^w[n]$, as readily seen from the exact expression

$$E_x^w[n] = \sum_{I=0}^{M-1} w_I \langle \Phi_I^w[n] | \hat{W}_{ee} | \Phi_I^w[n] \rangle - E_H[n]. \tag{10}$$

The minimum in eqn (5) is reached when the density n equals the exact ensemble one

$$n^w(r) = \sum_{I=0}^{M-1} w_I n_{\Psi_I}(r). \tag{11}$$

In practice, the minimising KS density matrix operator $\hat{\gamma}^w[n^w]$ can be determined from the following KS reformulation of the GOK variational principle,[49,78]

$$E^w = \min_{\hat{\Gamma}^w} \{ \mathrm{Tr}[\hat{\Gamma}^w (\hat{T} + \hat{V}_{ne})] + E_H[n_{\hat{\Gamma}^w}] + E_{xc}^w[n_{\hat{\Gamma}^w}] \}, \tag{12}$$

where $n_{\hat{\Gamma}^w}(r) = \sum_{I=0}^{M-1} w_I n_{\overline{\Psi}^{(I)}}$ is a trial ensemble density. As a result, the orbitals $\{\phi_p^w(r)\}_{1 \leq p \leq K}$ from which the KS wave functions $\{\Phi_I^w[n^w]\}_{0 \leq I \leq M-1}$ are constructed can be obtained by solving the following ensemble KS equation

$$\left\{ \hat{h}(r) + \frac{\delta E_{Hxc}^w[n^w]}{\delta n(r)} \right\} \phi_p^w(r) = \varepsilon_p^w \phi_p^w(r), \tag{13}$$

where $\hat{h}(r) = -\nabla^2/2 + v_{ne}(r)$, and

$$\frac{\delta E_{Hxc}^w[n]}{\delta n(r)} = \int \frac{n(r')}{|r - r'|} \mathrm{d}r' + \frac{\delta E_{xc}^w[n]}{\delta n(r)}. \tag{14}$$

The ensemble density can be obtained directly (and exactly, if no approximation is made) from these orbitals, *i.e.*,

$$n^w(r) = \sum_{I=0}^{M-1} w_I \left(\sum_p^K f_p^{(I)} \left[\phi_p^w(r) \right]^2 \right), \tag{15}$$

where $f_p^{(I)}$ denotes the occupation of $\phi_p^w(r)$ in the Ith KS wave function $\Phi_I^w[n^w]$. Turning to the excitation energies, they can be extracted from the density-functional ensemble as follows [see eqn (4) and (12) and ref. 46 and 49]:

$$\Omega^{(I)} = E_I^w - E_0^w + \left. \frac{\partial E_{xc}^w[n]}{\partial w_I} \right|_{n=n^w}, \tag{16}$$

where

$$E_I^w = \sum_p^K f_p^{(I)} \varepsilon_p^w \tag{17}$$

is the energy of the Ith KS state.

Eqn (16) is our working equation for computing excitation energies from a practical point of view. Note that the individual KS densities $n_{\Phi_I^w[n^w]}(r) = \sum_p^K f_p^{(I)} [\phi_p^w(r)]^2$ do not necessarily match the exact (interacting) individual-state densities $n_{\Psi_I}(r)$ as the non-interacting KS ensemble is expected to reproduce the true interacting ensemble density $n^w(r)$ defined in eqn (11), and not each individual density. Nevertheless, these densities can still be extracted in principle exactly from the KS ensemble as shown previously.[93]

In the following, we work at the (weight-dependent) ensemble LDA (eLDA) level of approximation, *i.e.*

$$E_{xc}^w[n] \underset{\approx}{\text{eLDA}} \int \varepsilon_{xc}^w(n(r))n(r)\mathrm{d}r, \tag{18}$$

$$\frac{\delta E_{xc}^w[n]}{\delta n(r)} \underset{\approx}{\text{eLDA}} \left.\frac{\partial \varepsilon_{xc}^w(n)}{\partial n}\right|_{n=n(r)} n(r) + \varepsilon_{xc}^w(n(r)). \tag{19}$$

We will also adopt the usual decomposition, and write down the weight-dependent xc functional as

$$\varepsilon_{xc}^w(n) = \varepsilon_x^w(n) + \varepsilon_c^w(n), \tag{20}$$

where $\varepsilon_x^w(n)$ and $\varepsilon_c^w(n)$ are the weight-dependent density-functional exchange and correlation energies per particle, respectively. As shown in Section IVA4, the weight dependence of the correlation energy can be extracted from an FUEG model. In order to make the resulting weight-dependent correlation functional truly universal, *i.e.*, independent on the number of electrons in the FUEG, one could use the curvature of the Fermi hole[89] as an additional variable in the density-functional approximation. The development of such a generalised correlation eLDA is left for future work. Even though a similar strategy could be applied to the weight-dependent exchange part, we explore in the present work a different path where the (system-dependent) exchange functional parameterisation relies on the ensemble energy linearity constraint (see Section IVA2). Finally, let us stress that, in order to further improve the description of the ensemble correlation energy, post-treatment of the recently revealed density-driven correlations[63,93–95] (which, by construction, are absent from FUEGs) might be necessary. An orbital-dependent correction as derived in ref. 93 might be used for that purpose. Work is currently in progress in this direction.

III. Computational details

The self-consistent GOK-DFT calculations [see eqn (13) and (15)] have been performed in a restricted formalism with the QuAcK software,[96] freely available on github, where the present weight-dependent functionals have been implemented. For more details about the self-consistent implementation of GOK-DFT, we refer the

interested reader to ref. 90 where additional technical details can be found. For all calculations, we use the aug-cc-pVXZ (X = D, T, Q, and 5) Dunning family of atomic basis sets.[97–99] Numerical quadratures are performed with the numgrid library[100] using 194 angular points (Lebedev grid) and a radial precision of 10^{-7}.[101,102]

This study deals only with spin-unpolarised systems, *i.e.*, $n_\uparrow = n_\downarrow = n/2$ (where $n_\uparrow$ and $n_\downarrow$ are the spin-up and spin-down electron densities). Moreover, we restrict our study to the case of a three-state ensemble (*i.e.*, $M = 3$) where the ground state ($I = 0$ with weight $1 - w_1 - w_2$), a singly-excited state ($I = 1$ with weight w_1), as well as the lowest doubly-excited state ($I = 2$ with weight w_2) are considered. Assuming that the singly-excited state is lower in energy than the doubly-excited state, one should have $0 \leq w_2 \leq 1/3$ and $w_2 \leq w_1 \leq (1 - w_2)/2$ to ensure the GOK variational principle. If the doubly-excited state (whose weight is denoted as w_2 throughout this work) is lower in energy than the singly-excited state (with weight w_1), which can be the case as one would notice later, then one has to swap w_1 and w_2 in the above inequalities. Note also that additional lower-in-energy single excitations may have to be included into the ensemble before incorporating the double excitation of interest. In the present exploratory work, we will simply exclude them from the ensemble and leave the more consistent (from a GOK point of view) description of all low-lying excitations to future work. Unless otherwise stated, we set the same weight to the two excited states (*i.e.*, $w \equiv w_1 = w_2$). In this case, the ensemble energy will be written as a single-weight quantity, E^w. The zero-weight limit (*i.e.*, $w \equiv w_1 = w_2 = 0$), and the equi-weight ensemble (*i.e.*, $w \equiv w_1 = w_2 = 1/3$) are considered in the following. (Note that the zero-weight limit corresponds to a conventional ground-state KS calculation.)

Let us finally mention that we will sometimes "violate" the GOK variational principle in order to build our weight-dependent functionals by considering the extended range of weights $0 \leq w_2 \leq 1$. The pure-state limit, $w_1 = 0 \wedge w_2 = 1$, is of particular interest as it is, like the (ground-state) zero-weight limit, a genuine saddle point of the restricted KS equations [see eqn (12) and (13)], and it matches perfectly the results obtained with the maximum overlap method (MOM) developed by Gilbert, Gill and coworkers.[103–105] From a GOK-DFT perspective, a (stationary) pure-excited-state limit can be seen as a way to construct density-functional approximations to individual exchange and state-driven correlations within an ensemble.[63,93,94] However, when it comes to compute excitation energies, we will exclusively consider ensembles where the largest weight is assigned to the ground state.

IV.   Results and discussion

In this section, we propose a two-step procedure to design, first, a weight- and system-dependent local exchange functional in order to remove some of the curvature of the ensemble energy. Second, we describe the construction of a universal, weight-dependent local correlation functional based on FUEGs. This procedure is applied to various two-electron systems in order to extract excitation energies associated with doubly-excited states.

A.   Hydrogen molecule at equilibrium

1.   Weight-independent exchange functional. First, we compute the ensemble energy of the H_2 molecule at equilibrium bond length (*i.e.*, $R_{H–H} = 1.4$ bohr) using

the aug-cc-pVTZ basis set and the conventional (weight-independent) LDA Slater exchange functional (*i.e.*, no correlation functional is employed),[106,107] which is explicitly given by

$$\varepsilon_x^S(n) = C_x n^{1/3}, \quad C_x = -\frac{3}{4}\left(\frac{3}{\pi}\right)^{1/3}. \tag{21}$$

In the case of H_2, the ensemble is composed of the ground state of electronic configuration $1\sigma_g^2$, the lowest singly-excited state of configuration $1\sigma_g 2\sigma_g$, and the lowest doubly-excited state of configuration $1\sigma_u^2$ (which has an auto-ionising resonance nature[108]) which all are of symmetry Σ_g^+. As mentioned previously, the lower-lying singly-excited states like $1\sigma_g 3\sigma_g$ and $1\sigma_g 4\sigma_g$, which should in principle be part of the ensemble (see Fig. 3 in ref. 109), have been excluded, for simplicity.

The deviation from linearity of the ensemble energy E^w [we recall that $w_1 = w_2 = w$] is depicted in Fig. 1 as a function of weight $0 \le w \le 1/3$ (blue curve). Because the Slater exchange functional defined in eqn (21) does not depend on the ensemble weight, there is no contribution from the ensemble derivative term [the last term in eqn (16)]. As anticipated, E^w is far from being linear, which means that the excitation energy associated with the doubly-excited state obtained *via* the derivative of the ensemble energy with respect to w_2 (and taken at $w_2 = w = w_1$) varies significantly with w (see blue curve in Fig. 2). Taking as a reference the full configuration interaction (FCI) value of 28.75 eV obtained with the aug-mcc-pV8Z basis set,[104] one can see that the excitation energy varies by more than 8 eV from $w = 0$ to $1/3$. Note that the exact xc ensemble functional would yield a perfectly linear ensemble energy and, hence, the same value of the excitation energy independent of the ensemble weights.

2. **Weight-dependent exchange functional.** Second, in order to remove some of this spurious curvature of the ensemble energy (which is mostly due to the ghost-interaction error,[51] with smaller effects from elsewhere[90]), one can easily reverse-engineer (for this particular system, geometry, basis set, and excitation) a local exchange functional to make $E^{(0,w_2)}$ as linear as possible for $0 \le w_2 \le 1$ assuming a perfect linearity between the pure-state limits $w_1 = w_2 = 0$ (ground state) and $w_1 = 0 \wedge w_2 = 1$ (doubly-excited state). In doing so, we have found that the following weight-dependent exchange functional (denoted as CC-S for "curvature-corrected" Slater functional)
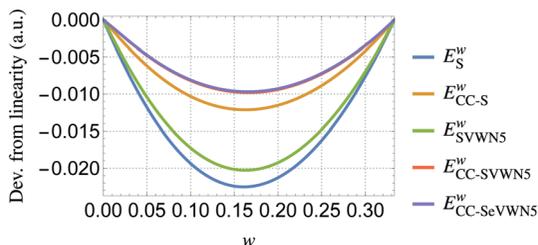
Fig. 1 H_2 at equilibrium bond length: deviation from linearity of the ensemble energy E^w (in hartree) as a function of w for various functionals and the aug-cc-pVTZ basis set. See main text for the definition of the various acronyms for the functionals.
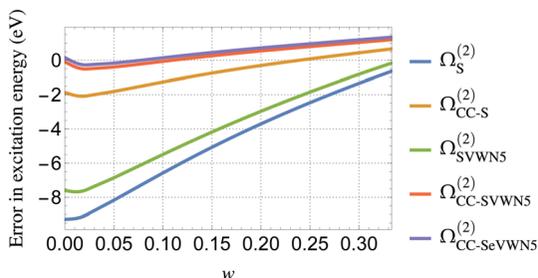
Fig. 2 H_2 at equilibrium bond length: error (with respect to FCI) in the excitation energy $\Omega^{(2)}$ (in eV) associated with the doubly-excited state as a function of w for various functionals and the aug-cc-pVTZ basis set. See main text for the definition of the various acronyms for the functionals.

$$\varepsilon_x^{w_2,\text{CC-S}}(n) = C_x^{w_2} n^{1/3}, \tag{22}$$

with

$$\frac{C_x^{w_2}}{C_x} = 1 - w_2(1 - w_2)\left[\alpha + \beta(w_2 - 1/2) + \gamma(w_2 - 1/2)^2\right], \tag{23}$$

and

$$\alpha = +0.575178,\ \beta = -0.021108,\ \gamma = -0.367189, \tag{24a}$$

makes the ensemble energy $E^{(0,w_2)}$ almost perfectly linear (by construction), and removes some of the curvature of E^w (see yellow curve in Fig. 1). It also allows "flattening of the curve", making the excitation energy much more stable (with respect to w), and closer to the FCI reference (see yellow curve in Fig. 2).

The parameters α, β, and γ entering eqn (23) have been obtained *via* a least-squares fit of the non-linear component of the ensemble energy computed between $w_2 = 0$ and $w_2 = 1$ by steps of 0.025. Although this range of weights is inconsistent with GOK theory, we have found that it is important, from a practical point of view, to ensure correct behaviour in the whole range of weights in order to obtain accurate excitation energies. Note that the CC-S functional depends on w_2 only, and not w_1, as it is specifically tuned for the double excitation. Hence, only the double excitation includes a contribution from the ensemble derivative term [see eqn (16)].

The present procedure can be related to optimally-tuned range-separated hybrid functionals,[110] where the range-separation parameters (which control the amount of short- and long-range exact exchange) are determined individually for each system by iteratively tuning them in order to enforce non-empirical conditions related to frontier orbitals (*e.g.*, ionisation potential, electron affinity, *etc.*) or, more importantly here, the piecewise linearity of the ensemble energy for ensemble states described by a fractional number of electrons.[110–113] In this context, the analog of the "ionisation potential theorem" for the first (neutral) excitation, for example, would read as follows [see eqn (1), (4) and (16)]:

$$2\left(E^{w_1=1/2} - E^{w_1=0}\right) \overset{0 \leq w_1 \leq 1/2}{=} E_1^{w_1} - E_0^{w_1} + \left.\frac{\partial E_{xc}^{w_1}[n]}{\partial w_1}\right|_{n=n^{w_1}} \tag{25}$$
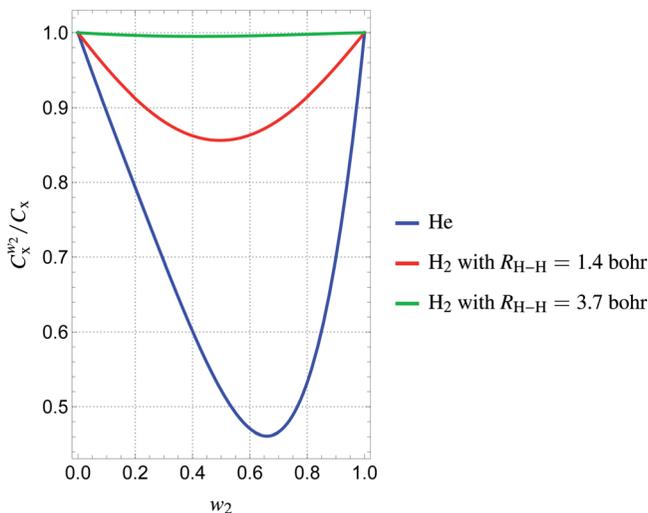
Fig. 3 $C_x^{w_2}/C_x$ as a function of w_2 [see eqn (23)] computed with the aug-cc-pVTZ basis set for the He atom (blue) and the H_2 molecule at $R_{H-H} = 1.4$ bohr (red), and $R_{H-H} = 3.7$ bohr (green).

We enforce this type of exact constraint (to the maximum possible extent) when optimising the parameters in eqn (23) in order to minimise the curvature of the ensemble energy. As readily seen from eqn (23) and graphically illustrated in Fig. 3 (red curve), the weight-dependent correction does not affect the two ghost-interaction-free limits at $w_1 = w_2 = 0$ and $w_1 = 0 \wedge w_2 = 1$ (*i.e.*, the pure-state limits), as $C_x^{w_2}$ reduces to C_x in these two limits. Indeed, it is important to ensure that the weight-dependent functional does not alter these pure-state limits, which are genuine saddle points of the KS equations, as mentioned above. Finally, let us mention that, around $w_2 = 0$, the behaviour of eqn (23) is linear: this is the main feature that one needs to catch in order to get accurate excitation energies in the zero-weight limit which is ghost-interaction free. Nonetheless, beyond the $w_2 = 0$ limit, the CC-S functional also includes quadratic terms in order to compensate the spurious curvature of the ensemble energy originating, mainly, from the Hartree term [see eqn (9)].

3.   **Weight-independent correlation functional.** Third, we include correlation effects *via* the conventional VWN5 local correlation functional.[114] For the sake of clarity, the explicit expression of the VWN5 functional is not reported here but it can be found in ref. 114. The combination of the (weight-independent) Slater and VWN5 functionals (SVWN5) yield a highly convex ensemble energy (green curve in Fig. 1), while the combination of CC-S and VWN5 (CC-SVWN5) exhibits a smaller curvature and improved excitation energies (red curve in Fig. 1 and 2), especially at small weights, where the CC-SVWN5 excitation energy is almost spot on.

4.   **Weight-dependent correlation functional.** Fourth, in the spirit of our recent work,[90] we design a universal, weight-dependent correlation functional. To build this correlation functional, we consider the singlet ground state, the first singly-excited state, as well as the first doubly-excited state of two-electron FUEGs which consists of two electrons confined to the surface of a 3-sphere (also known

as a glome).[115–117] Notably, these three states have the same (uniform) density $n = 2/(2\pi^2 R^3)$, where R is the radius of the 3-sphere onto which the electrons are confined. Note that the present paradigm is equivalent to the conventional IUEG model in the thermodynamic limit.[85] We refer the interested reader to ref. 85 and 89 for more details about this paradigm.

The reduced (i.e., per electron) Hartree–Fock (HF) energies for these three states are

$$\varepsilon_{\mathrm{HF}}^{(0)}(n) = \frac{4}{3}\left(\frac{n}{\pi}\right)^{1/3}, \tag{26a}$$

$$\varepsilon_{\mathrm{HF}}^{(1)}(n) = \frac{3\pi^2}{4}\left(\frac{n}{\pi}\right)^{2/3} + \frac{16}{10}\left(\frac{n}{\pi}\right)^{1/3}. \tag{26b}$$

$$\varepsilon_{\mathrm{HF}}^{(2)}(n) = \frac{3\pi^2}{2}\left(\frac{n}{\pi}\right)^{2/3} + \frac{176}{105}\left(\frac{n}{\pi}\right)^{1/3}. \tag{26c}$$

Thanks to highly-accurate calculations[115–117] and the expressions of the HF energies provided by eqn (26a)–(26c), one can write down, for each state, an accurate analytical expression of the reduced correlation energy[87,118] via the following simple Padé approximant[90,119]

$$\varepsilon_{\mathrm{c}}^{(I)}(n) = \frac{a_1^{(I)}}{1 + a_2^{(I)} n^{-1/6} + a_3^{(I)} n^{-1/3}}, \tag{27}$$

where $a_2^{(I)}$ and $a_3^{(I)}$ are state-specific fitting parameters, which are provided in Table 2. The value of $a_1^{(I)}$ is obtained via the exact high-density expansion of the correlation energy.[85] Eqn (27) is depicted in Fig. 4 for each state alongside the data
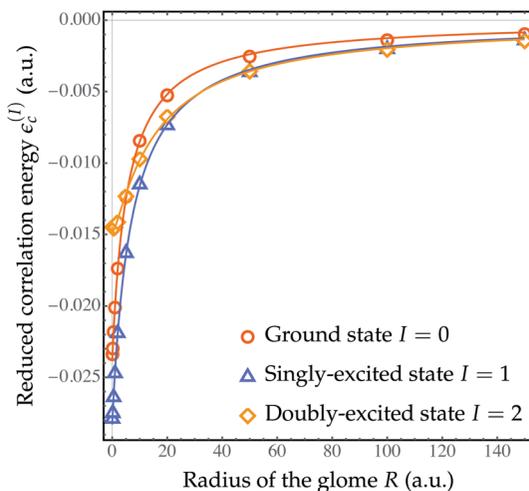
Fig. 4 Reduced (i.e., per electron) correlation energy $\varepsilon_c^{(I)}$ [see eqn (27)] as a function of $R = 1/(\pi^2 n)^{1/3}$ for the ground state ($I = 0$), the first singly-excited state ($I = 1$), and the first doubly-excited state ($I = 2$) of the two-electron FUEG. The data are also gathered in Table 1.

Table 1 $-\varepsilon_c^{(I)}$ as a function of the radius of the glome $R = 1/(\pi^2 n)^{1/3}$ for the ground state ($I = 0$), the first singly-excited state ($I = 1$), and the first doubly-excited state ($I = 2$) of the two-electron FUEG

R	Ground state $I = 0$	Single excitation $I = 1$	Double excitation $I = 2$
0	0.023818	0.028281	0.014463
0.1	0.023392	0.027886	0.014497
0.2	0.022979	0.027499	0.014523
0.5	0.021817	0.026394	0.014561
1	0.020109	0.024718	0.014512
2	0.017371	0.021901	0.014142
5	0.012359	0.016295	0.012334
10	0.008436	0.011494	0.009716
20	0.005257	0.007349	0.006744
50	0.002546	0.003643	0.003584
100	0.001399	0.002025	0.002059
150	0.000972	0.001414	0.001458

Table 2 Parameters of the correlation functionals for each individual state defined in eqn (27). The values of a_1 are obtained to reproduce the exact high density correlation energy of each individual state, while a_2 and a_3 are fitted on the numerical values reported in Table 1

	Ground state $I =$ 0	Single excitation $I = 1$	Double excitation $I = 2$
a_1	−0.0238184	−0.0282814	−0.0144633
a_2	+0.00540994	+0.00273925	−0.0506020
a_3	+0.0830766	+0.0664914	+0.0331417

gathered in Table 1. Combining these, we build a three-state weight-dependent correlation functional:

$$\varepsilon_c^w(n) = (1 - w_1 - w_2)\varepsilon_c^{(0)}(n) + w_1\varepsilon_c^{(1)}(n) + w_2\varepsilon_c^{(2)}(n), \tag{28}$$

where, unlike in the exact theory,[93] the individual components are weight independent.

Because our intent is to incorporate into standard functionals (which are "universal" in the sense that they do not depend on the number of electrons), information about excited states that will be extracted from finite systems (whose properties may depend on the number of electrons), we employ a simple "embedding" scheme where the two-electron FUEG (the impurity) is embedded in the IUEG (the bath). As explained further in ref. 90, this embedding procedure can be theoretically justified by the generalised adiabatic connection formalism for ensembles originally derived by Franck and Fromager.[52] The weight-dependence of the correlation functional is then carried exclusively by the impurity [*i.e.*, the functional defined in eqn (28)], while the remaining effects are produced by the bath (*i.e.*, the usual ground-state LDA correlation functional).

Consistently with such a strategy, eqn (28) is "centred" on its corresponding weight-independent VWN5 LDA reference

$$\varepsilon_c^{w,\text{eVWN5}}(n) = (1 - w_1 - w_2)\bar{\varepsilon}_c^{(0)}(n) + w_1\bar{\varepsilon}_c^{(1)}(n) + w_2\bar{\varepsilon}_c^{(2)}(n) \tag{29}$$

via the following global, state-independent shift:

$$\bar{\varepsilon}_c^{(I)}(n) = \varepsilon_c^{(I)}(n) + \varepsilon_c^{\text{VWN5}}(n) - \varepsilon_c^{(0)}(n). \tag{30}$$

In the following, we name this weight-dependent correlation functional "eVWN5" as it is a natural extension of the VWN5 local correlation functional for ensembles. Also, eqn (29) can be recast as

$$\begin{aligned} \varepsilon_c^{w,\text{eVWN5}}(n) = \varepsilon_c^{\text{eVWN5}}(n) \\ + w_1\left[\varepsilon_c^{(1)}(n) - \varepsilon_c^{(0)}(n)\right] + w_2\left[\varepsilon_c^{(2)}(n) - \varepsilon_c^{(0)}(n)\right] \end{aligned} \tag{31}$$

which nicely highlights the centrality of VWN5 in the present weight-dependent density-functional approximation for ensembles. In particular, $\varepsilon_c^{(0,0),\text{eVWN5}}(n) = \varepsilon_c^{\text{VWN5}}(n)$. We note also that, by construction, we have

$$\frac{\partial\varepsilon_c^{w,\text{eVWN5}}(n)}{\partial w_I} = \varepsilon_c^{(I)}(n) - \varepsilon_c^{(0)}(n), \tag{32}$$

showing that the weight correction is purely linear in eVWN5 and entirely dependent on the FUEG model. Contrary to the CC-S exchange functional which only depends on w_2, the eVWN5 correlation functional depends on both weights.

As shown in Fig. 1, the CC-SeVWN5 ensemble energy (as a function of w) is very slightly less concave than its CC-SVWN5 counterpart and it also improves (not by much) the excitation energy (see purple curve in Fig. 2).

For a more qualitative picture, Table 3 reports the excitation energies for various methods and basis sets. In particular, we report the excitation energies obtained with GOK-DFT in the zero-weight limit (*i.e.*, $w = 0$) and for equi-weights (*i.e.*, $w = 1/3$). These excitation energies are computed using eqn (16).

For comparison, we also report results obtained with the linear interpolation method (LIM).[78,79] The latter simply consists of extracting the excitation energies (which are weight-independent, by construction) from the equi-ensemble energies, as follows:

$$\Omega_{\text{LIM}}^{(1)} = 2[E^{w=(1/2,0)} - E^{w=(0,0)}], \tag{33a}$$

$$\Omega_{\text{LIM}}^{(2)} = 3\left[E^{w=(1/3,1/3)} - E^{w=(1/2,0)}\right] + \frac{1}{2}\Omega_{\text{LIM}}^{(1)}. \tag{33b}$$

For a general expression with multiple (and possibly degenerate) states, we refer the reader to eqn (106) of ref. 78, where LIM is shown to interpolate linearly with the ensemble energy between equi-ensembles. Note that two calculations are needed to get the first LIM excitation energy, with an additional equi-ensemble calculation for each higher excitation energy.

Additionally, MOM excitation energies[103–105]

$$\Omega_{\text{MOM}}^{(1)} = E^{w=(1,0)} - E^{w=(0,0)}, \tag{34a}$$

Table 3 Excitation energies (in eV) associated with the lowest double excitation of H_2 with $R_{H-H} = 1.4$ bohr for various methods, combinations of xc functionals, and basis sets

xc functional			GOK			
x	c	Basis	$w = 0$	$w = 1/3$	LIM[a]	MOM[a]
HF		aug-cc-pVDZ	35.59	33.33		28.65
		aug-cc-pVTZ	35.01	33.51		28.65
		aug-cc-pVQZ	34.66	33.54		28.65
HF	VWN5	aug-cc-pVDZ	37.83	33.86		29.17
		aug-cc-pVTZ	37.61	33.99		29.17
		aug-cc-pVQZ	37.07	34.01		29.17
HF	eVWN5	aug-cc-pVDZ	38.09	34.00		29.34
		aug-cc-pVTZ	37.61	34.13		29.34
		aug-cc-pVQZ	37.32	34.14		29.34
S		aug-cc-pVDZ	19.44	28.00	25.09	26.60
		aug-cc-pVTZ	19.47	28.11	25.20	26.67
		aug-cc-pVQZ	19.41	28.13	25.22	26.67
S	VWN5	aug-cc-pVDZ	21.04	28.49	25.90	27.10
		aug-cc-pVTZ	21.14	28.58	25.99	27.17
		aug-cc-pVQZ	21.13	28.59	26.00	27.17
S	eVWN5	aug-cc-pVDZ	21.28	28.64	25.99	27.27
		aug-cc-pVTZ	21.39	28.74	26.08	27.34
		aug-cc-pVQZ	21.38	28.75	26.09	27.34
CC-S		aug-cc-pVDZ	26.83	29.29	28.83	26.60
		aug-cc-pVTZ	26.88	29.41	28.96	26.67
		aug-cc-pVQZ	26.82	29.43	28.97	26.67
CC-S	VWN5	aug-cc-pVDZ	28.54	29.85	29.73	27.10
		aug-cc-pVTZ	28.66	29.96	29.83	27.17
		aug-cc-pVQZ	28.64	29.97	29.84	27.17
CC-S	eVWN5	aug-cc-pVDZ	28.78	29.99	29.82	27.27
		aug-cc-pVTZ	28.90	30.10	29.92	27.34
		aug-cc-pVQZ	28.89	30.11	29.93	27.34
B	LYP	aug-mcc-pV8Z				28.42
B3	LYP	aug-mcc-pV8Z				27.77
HF	LYP	aug-mcc-pV8Z				29.18
HF		aug-mcc-pV8Z				28.65
Accurate[b]						28.75

[a] Eqn (33b) and (34b) are used where the first weight corresponds to the singly-excited state.
[b] FCI/aug-mcc-pV8Z calculation from ref. 104.

$$\Omega^{(2)}_{MOM} = E^{w=(0,1)} - E^{w=(0,0)}, \tag{34b}$$

which also require three separate calculations at a different set of ensemble weights, have been computed for further comparison.

As readily seen in eqn (33a) and (33b), LIM is a recursive strategy where the first excitation energy has to be determined in order to compute the second one. In the above equations, we assumed that the singly-excited state (with weight w_1) is lower in energy than the doubly-excited state (with weight w_2). If the ordering changes (like in the case of the stretched H_2 molecule, see below), one should substitute $E^{w=(0,1/2)}$ by $E^{w=(1/2,0)}$ in eqn (33a) and (33b) which then correspond to the excitation energies of the doubly-excited and singly-excited states, respectively. The same holds for the MOM excitation energies in eqn (34a) and (34b).

The results gathered in Table 3 show that the GOK-DFT excitation energies obtained with the CC-SeVWN5 functional at zero weight are the most accurate with an improvement of 0.25 eV as compared to CC-SVWN5, which is due to the ensemble derivative contribution of the eVWN5 functional. The CC-SeVWN5 excitation energies at equi-weights (*i.e.*, $w = 1/3$) are less satisfactory, but still remain in good agreement with FCI. Interestingly, the CC-S functional leads to a substantial improvement of the LIM excitation energy, getting closer to the reference value when no correlation functional is used. When correlation functionals are added (*i.e.*, VWN5 or eVWN5), LIM tends to overestimate the excitation energy by about 1 eV but still performs better than when no correction of the curvature is considered. It is also important to mention that the CC-S functional does not alter the MOM excitation energy as the correction vanishes in this limit (*vide supra*). Finally, although we had to design a system-specific, weight-dependent exchange functional to reach such accuracy, we have not used any high-level reference data (such as FCI) to tune our functional, the only requirement being the linearity of the ensemble energy (obtained with LDA exchange) between the ghost-interaction-free pure-state limits.

B.   Hydrogen molecule at stretched geometry

To investigate the weight dependence of the xc functional in the strong correlation regime, we now consider the H_2 molecule in a stretched geometry ($R_{H-H} = 3.7$ bohr). Note that, for this particular geometry, the doubly-excited state becomes the lowest excited state with the same symmetry as the ground state. Although we could safely restrict ourselves to a bi-ensemble composed of the ground state and the doubly-excited state, we eschew doing this and still consider the same tri-ensemble defined in Section IVA. Nonetheless, one should just be careful when reading the equations reported above, as they correspond to the case where the singly-excited state is lower in energy than the doubly-excited state. We then follow the same protocol as in Section IVA, and considering again the aug-cc-pVTZ basis set, we design a CC-S functional for this system at $R_{H-H} = 3.7$ bohr. It yields $\alpha = +0.019226$, $\beta = -0.017996$, and $\gamma = -0.022945$ [see eqn (23)]. The weight dependence of $C_x^{w_2}$ is illustrated in Fig. 3 (green curve).

One clearly sees that the correction brought by CC-S is much more gentle than at $R_{H-H} = 1.4$ bohr, which means that the ensemble energy obtained with the LDA exchange functional is much more linear at $R_{H-H} = 3.7$ bohr. Note that this linearity at $R_{H-H} = 3.7$ bohr was also observed using the weight-independent xc functionals in ref. 78. Table 4 reports, for the aug-cc-pVTZ basis set (which delivers basis set converged results), the same set of calculations as in Table 3. As a reference value, we computed a FCI/aug-cc-pV5Z excitation energy of 8.69 eV, which compares well with previous studies.[78] For $R_{H-H} = 3.7$ bohr, it is much harder to get an accurate estimate of the excitation energy, the closest match being reached with HF exchange and VWN5 correlation at equi-weights. As expected from the linearity of the ensemble energy, the CC-S functional coupled or not with a correlation functional yield extremely stable excitation energies as a function of the weight, with only a few tenths of eV difference between the zero- and equi-weight limits. As a direct consequence of this linearity, LIM and MOM do not provide any noticeable improvement on the excitation energy. Nonetheless, the excitation energy is still off by 3 eV. The fundamental theoretical reason

Table 4 Excitation energies (in eV) associated with the lowest double excitation of H_2 at $R_{H-H} = 3.7$ bohr obtained with the aug-cc-pVTZ basis set for various methods and combinations of xc functionals

xc functional		GOK			
x	c	$w = 0$	$w = 1/3$	LIM[a]	MOM[a]
HF		19.09	8.82	12.92	6.52
HF	VWN5	19.40	8.81	13.02	6.49
HF	eVWN5	19.59	8.95	13.11	[b]
S		5.31	5.67	5.46	5.56
S	VWN5	5.34	5.64	5.46	5.52
S	eVWN5	5.53	5.79	5.56	5.72
CC-S		5.55	5.72	5.56	5.56
CC-S	VWN5	5.58	5.69	5.57	5.52
CC-S	eVWN5	5.77	5.84	5.66	5.72
B	LYP				5.28
B3	LYP				5.55
HF	LYP				6.68
srLDA ($\mu = 0.4$)[c]		6.39		6.47	
Accurate[d]					8.69

[a] Eqn (33a) and (34a) are used where the first weight corresponds to the doubly-excited state. [b] KS calculation does not converge. [c] Short-range multiconfigurational DFT/aug-cc-pVQZ calculations from ref. 78. [d] FCI/aug-cc-pV5Z calculation performed with QUANTUM PACKAGE.[121]

for such poor agreement is not clear but it might be that, in this strongly correlated regime, the weight-dependent correlation functional plays a significant role not caught by our approximation.

For additional comparison, we provide the excitation energy calculated by short-range multiconfigurational DFT in ref. 78, using the (weight-independent) srLDA functional[120] and setting the range-separation parameter to $\mu = 0.4$ bohr^{-1}. The excitation energy improves by 1 eV compared to the weight-independent SVWN5 functional, thus showing that treating the long-range part of the electron–electron repulsion by wave function theory plays a significant role.

C. Helium atom

As a final example, we consider the He atom which can be seen as the limiting form of the H_2 molecule for very short bond lengths. Similar to H_2, our ensemble contains the ground state of configuration $1s^2$, the lowest singlet excited state of configuration $1s2s$, and the first doubly-excited state of configuration $2s^2$. In He, the lowest doubly-excited state is an auto-ionising resonance state, extremely high in energy and lies in the continuum.[122] In ref. 123, highly-accurate calculations estimate an excitation energy of 2.126 hartree for this $1s^2 \rightarrow 2s^2$ transition. Nonetheless, it can be nicely described with a Gaussian basis set containing enough diffuse functions. Consequently, we consider for this particular example the d-aug-cc-pVQZ basis set which contains two sets of diffuse functions. The excitation energies associated with this double excitation computed with various methods and combinations of xc functionals are gathered in Table 5.

Table 5 Excitation energies (in hartree) associated with the lowest double excitation of He obtained with the d-aug-cc-pVQZ basis set for various methods and combinations of xc functionals

xc functional		GOK			
x	c	$w = 0$	$w = 1/3$	LIM[a]	MOM[a]
HF		1.874	2.212	2.123	2.142
HF	VWN5	1.988	2.260	2.190	2.193
HF	eVWN5	2.000	2.265	2.193	2.196
S		1.062	2.056	1.675	2.030
S	VWN5	1.163	2.104	1.735	2.079
S	eVWN5	1.174	2.109	1.738	2.083
CC-S		1.996	2.264	2.148	2.030
CC-S	VWN5	2.107	2.318	2.215	2.079
CC-S	eVWN5	2.108	2.323	2.218	2.083
B	LYP				2.147
B3	LYP				2.150
HF	LYP				2.171
Accurate[b]					2.126

[a] Eqn (33b) and (34b) are used where the first weight corresponds to the singly-excited state.
[b] Explicitly-correlated calculations from ref. 123.

Before analysing the results, we would like to highlight the fact that there is a large number of singly-excited states lying between the 1s2s and $2s^2$ states. Therefore, the present ensemble is not consistent with GOK theory. However, it is impossible, from a practical point of view, to take into account all these single excitations. We then restrict ourselves to a tri-ensemble keeping in mind the possible theoretical loopholes of such a choice.

The parameters of the CC-S weight-dependent exchange functional (computed with the smaller aug-cc-pVTZ basis) are $\alpha = +1.912574$, $\beta = +2.715267$, and $\gamma = +2.163422$ [see eqn (23)], with the curvature of the ensemble energy being more pronounced in He than in H_2 (blue curve in Fig. 3). The results reported in Table 5 evidence this strong weight dependence of the excitation energies for HF or LDA exchange.

The CC-S exchange functional attenuates significantly this dependence, and when coupled with the eVWN5 weight-dependent correlation functional, the CC-SeVWN5 excitation energy at $w = 0$ is only 18 millihartree off the reference value. As in the case of H_2, the excitation energies obtained at zero-weight are more accurate than at equi-weight, while the opposite conclusion was made in ref. 90. This highlights further the importance of developing weight-dependent functionals that yields linear ensemble energies in order to get rid of the weight-dependency of the excitation energy. Here again, the LIM excitation energy using the CC-S functional is very accurate with only a 22 millihartree error compared to the reference value, while adding the correlation contribution to the functional tends to overestimate the excitation energy. Hence, in light of the results obtained in this paper, it seems that the weight-dependent curvature correction to the exchange functional has the largest impact on the accuracy of the excitation energies.

As a final comment, let us stress again that the present protocol does not rely on high-level calculations, as the sole requirement for constructing the CC-S functional is the linearity of the ensemble energy with respect to the weight of the double excitation.

V.   Conclusion

In the present article, we have discussed the construction of first-rung (*i.e.*, local) weight-dependent exchange–correlation density-functional approximations for two-electron systems (He and H_2), specifically designed for the computation of double excitations within GOK-DFT, a time-independent formalism capable of extracting excitation energies *via* the derivative of the ensemble energy with respect to the weight of each excited state.

In the spirit of optimally-tuned range-separated hybrid functionals, we have found that the construction of a system- and excitation-specific weight-dependent local exchange functional can significantly reduce the curvature of the ensemble energy and improve excitation energies. The present weight-dependent exchange functional, CC-S, specifically tailored for double excitations, only depends on the weight of the doubly-excited state, CC-S being independent of the weight of the singly-excited state. We are currently investigating a generalisation of the present procedure in order to include a dependency on both weights in the exchange functional.

Although the weight-dependent correlation functional developed in this paper (eVWN5) performs systematically better than the weight-independent counterpart (VWN5), the improvement remains rather small. To better understand the reasons behind this, it would be particularly interesting to investigate the influence of the self-consistent procedure, *i.e.*, the variation in excitation energy when the exact ensemble density (built with the exact individual densities) is used, instead of the self-consistent one. Exploring the impact of both density- and state-driven correlations[63,93,94] may provide additional insight into the present results. This is left for future work.

In light of the results obtained in this study on double excitations computed within the GOK-DFT framework, we believe that the development of more universal weight-dependent exchange and correlation functionals has a bright future, and we hope to be able to report further on this in the near future.

Conflicts of interest

There are no conflicts to declare.

Acknowledgements

References

1 M. E. Casida, *Time-dependent density functional response theory for molecules*, World Scientific, Singapore, 1995, pp. 155–192.

2 C. Ullrich, *Time-Dependent Density-Functional Theory: Concepts and Applications*, Oxford Graduate Texts (Oxford University Press), New York, 2012.

3 P. F. Loos, A. Scemama and D. Jacquemin, *J. Phys. Chem. Lett.*, 2020, **11**, 974.

4 A. Dreuw and M. Head-Gordon, *Chem. Rev.*, 2005, **105**, 4009.

5 P. Hohenberg and W. Kohn, *Phys. Rev.*, 1964, **136**, B864.

6 W. Kohn and L. J. Sham, *Phys. Rev.*, 1965, **140**, A1133.

7 R. G. Parr and W. Yang, *Density-functional theory of atoms and molecules*, Clarendon Press, Oxford, 1989.

8 E. Runge and E. K. U. Gross, *Phys. Rev. Lett.*, 1984, **52**, 997.

9 M. Casida and M. Huix-Rotllant, *Annu. Rev. Phys. Chem.*, 2012, **63**, 287.

10 G. Vignale, *Phys. Rev. A: At., Mol., Opt. Phys.*, 2008, **77**, 062511.

11 D. J. Tozer, R. D. Amos, N. C. Handy, B. O. Roos and L. Serrano-Andres, *Mol. Phys.*, 1999, **97**, 859.

12 A. Dreuw, J. L. Weisman and M. Head-Gordon, *J. Chem. Phys.*, 2003, **119**, 2943.

13 A. L. Sobolewski and W. Domcke, *Chem. Phys.*, 2003, **294**, 73.

14 A. Dreuw and M. Head-Gordon, *J. Am. Chem. Soc.*, 2004, **126**, 4007.

15 N. T. Maitra, *J. Phys.: Condens. Matter*, 2017, **29**, 423001.

16 D. J. Tozer and N. C. Handy, *J. Chem. Phys.*, 1998, **109**, 10180.

17 D. J. Tozer and N. C. Handy, *Phys. Chem. Chem. Phys.*, 2000, **2**, 2117.

18 M. E. Casida, C. Jamorski, K. C. Casida and D. R. Salahub, *J. Chem. Phys.*, 1998, **108**, 4439.

19 M. E. Casida and D. R. Salahub, *J. Chem. Phys.*, 2000, **113**, 8918.

20 D. J. Tozer, *J. Chem. Phys.*, 2003, **119**, 12697.

21 Y. Tawada, T. Tsuneda, S. Yanagisawa, T. Yanai and K. Hirao, *J. Chem. Phys.*, 2004, **120**, 8425.

22 T. Yanai, D. P. Tew and N. C. Handy, *Chem. Phys. Lett.*, 2004, **393**, 51.

23 B. G. Levine, C. Ko, J. Quenneville and T. J. MartÍnez, *Mol. Phys.*, 2006, **104**, 1039.

24 P. Elliott, S. Goldson, C. Canahui and N. T. Maitra, *Chem. Phys.*, 2011, **391**, 110.

25 M. Boggio-Pasqua, M. J. Bearpark and M. A. Robb, *J. Org. Chem.*, 2007, **72**, 4497.

26 P. F. Loos, A. Scemama, A. Blondel, Y. Garniron, M. Caffarel and D. Jacquemin, *J. Chem. Theory Comput.*, 2018, **14**, 4360.

27 P.-F. Loos, M. Boggio-Pasqua, A. Scemama, M. Caffarel and D. Jacquemin, *J. Chem. Theory Comput.*, 2019, **15**, 1939.

28 P. F. Loos, F. Lipparini, M. Boggio-Pasqua, A. Scemama and D. Jacquemin, *J. Chem. Theory Comput.*, 2020, **16**, 1711.

29 M. Huix-Rotllant, B. Natarajan, A. Ipatov, C. Muhavini Wawire, T. Deutsch and M. E. Casida, *Phys. Chem. Chem. Phys.*, 2010, **12**, 12811.

30 A. I. Krylov, *Chem. Phys. Lett.*, 2001, **350**, 522.

31 Y. Shao, M. Head-Gordon and A. I. Krylov, *J. Chem. Phys.*, 2003, **118**, 4807.

32 F. Wang and T. Ziegler, *J. Chem. Phys.*, 2004, **121**, 12191.

33 F. Wang and T. Ziegler, *Int. J. Quantum Chem.*, 2006, **106**, 2545.

34 N. Minezawa and M. S. Gordon, *J. Phys. Chem. A*, 2009, **113**, 12749.

35 S. Lee, M. Filatov, S. Lee and C. H. Choi, *J. Chem. Phys.*, 2018, **149**, 104101.

36 N. T. Maitra, F. Zhang, R. J. Cave and K. Burke, *J. Chem. Phys.*, 2004, **120**, 5932.

37 R. J. Cave, F. Zhang, N. T. Maitra and K. Burke, *Chem. Phys. Lett.*, 2004, **389**, 39.

38 G. Mazur and R. Włodarczyk, *J. Comput. Chem.*, 2009, **30**, 811.

39 G. Mazur, M. Makowski, R. Włodarczyk and Y. Aoki, *Int. J. Quantum Chem.*, 2011, **111**, 819.

40 M. Huix-Rotllant, A. Ipatov, A. Rubio and M. E. Casida, *Chem. Phys.*, 2011, **391**, 120.

41 N. T. Maitra, Memory: history, initial-state dependence, and double-excitations, in *Fundamentals of Time-Dependent Density Functional Theory*, ed. M. A. Marques, N. T. Maitra, F. M. Nogueira, E. Gross and A. Rubio, Springer Berlin Heidelberg, Berlin, Heidelberg, 2012, vol. 837, pp. 167–184.

42 P. Romaniello, D. Sangalli, J. A. Berger, F. Sottile, L. G. Molinari, L. Reining and G. Onida, *J. Chem. Phys.*, 2009, **130**, 044108.

43 D. Sangalli, P. Romaniello, G. Onida and A. Marini, *J. Chem. Phys.*, 2011, **134**, 034115.

44 Z.-H. Yang, A. Pribram-Jones, K. Burke and C. A. Ullrich, *Phys. Rev. Lett.*, 2017, **119**, 033003.

45 F. Sagredo and K. Burke, *J. Chem. Phys.*, 2018, **149**, 134103.

46 K. Deur and E. Fromager, *J. Chem. Phys.*, 2019, **150**, 094106.

47 A. K. Theophilou, *J. Phys. C: Solid State Phys.*, 1979, **12**, 5419.

48 E. K. U. Gross, L. N. Oliveira and W. Kohn, *Phys. Rev. A: At., Mol., Opt. Phys.*, 1988, **37**, 2805.

49 E. K. U. Gross, L. N. Oliveira and W. Kohn, *Phys. Rev. A: At., Mol., Opt. Phys.*, 1988, **37**, 2809.

50 L. N. Oliveira, E. K. U. Gross and W. Kohn, *Phys. Rev. A: At., Mol., Opt. Phys.*, 1988, **37**, 2821.

51 N. I. Gidopoulos, P. G. Papaconstantinou and E. K. U. Gross, *Phys. Rev. Lett.*, 2002, **88**, 033003.

52 O. Franck and E. Fromager, *Mol. Phys.*, 2014, **112**, 1684.

53 A. Borgoo, A. M. Teale and T. Helgaker, *AIP Conf. Proc.*, 2015, **1702**, 090049.

54 A. Kazaryan, J. Heuver and M. Filatov, *J. Phys. Chem. A*, 2008, **112**, 12980.

55 T. Gould and J. F. Dobson, *J. Chem. Phys.*, 2013, **138**, 014103.

56 T. Gould and J. Toulouse, *Phys. Rev. A: At., Mol., Opt. Phys.*, 2014, **90**, 050502.

57 M. Filatov, M. Huix-Rotllant and I. Burghardt, *J. Chem. Phys.*, 2015, **142**, 184104.

58 M. Filatov, Ensemble DFT Approach to Excited States of Strongly Correlated Molecular Systems, in *Density-Functional Methods for Excited States*, ed. N. Ferré, M. Filatov and M. Huix-Rotllant, Springer International Publishing, Cham, 2015, vol. 368, pp. 97–124.

59 M. Filatov, *Wiley Interdiscip. Rev.: Comput. Mol. Sci.*, 2015, **5**, 146.

60 T. Gould and S. Pittalis, *Phys. Rev. Lett.*, 2017, **119**, 243001.

61 K. Deur, L. Mazouin and E. Fromager, *Phys. Rev. B*, 2017, **95**, 035120.

62 T. Gould, L. Kronik and S. Pittalis, *J. Chem. Phys.*, 2018, **148**, 174101.

63 T. Gould and S. Pittalis, *Phys. Rev. Lett.*, 2019, **123**, 016401.

64 P. W. Ayers, M. Levy and A. Nagy, *Theor. Chem. Acc.*, 2018, **137**, 152.

65 K. Deur, L. Mazouin, B. Senjean and E. Fromager, *Eur. Phys. J. B*, 2018, **91**, 162.

66 E. Kraisler and L. Kronik, *Phys. Rev. Lett.*, 2013, **110**, 126403.

67 E. Kraisler and L. Kronik, *J. Chem. Phys.*, 2014, **140**, 18A540.

68 M. M. Alam, S. Knecht and E. Fromager, *Phys. Rev. A*, 2016, **94**, 012511.

69 M. M. Alam, K. Deur, S. Knecht and E. Fromager, *J. Chem. Phys.*, 2017, **147**, 204105.

70 A. Nagy, *Int. J. Quantum Chem.*, 1998, **69**, 247.

71 A. Nagy, *J. Phys. B: At., Mol. Opt. Phys.*, 2001, **34**, 2363.

72 A. Nagy, S. Liu and L. Bartolloti, *J. Chem. Phys.*, 2005, **122**, 134107.

73 E. Pastorczak, N. I. Gidopoulos and K. Pernal, *Phys. Rev. A: At., Mol., Opt. Phys.*, 2013, **87**, 062501.

74 E. Pastorczak and K. Pernal, *J. Chem. Phys.*, 2014, **140**, 18A514.

75 A. Pribram-Jones, Z.-h. Yang, J. R. Trail, K. Burke, R. J. Needs and C. A. Ullrich, *J. Chem. Phys.*, 2014, **140**, 18A541.

76 W. Yang, P. Mori-Sánchez and A. J. Cohen, *J. Chem. Phys.*, 2013, **139**, 104114.

77 Z.-H. Yang, J. R. Trail, A. Pribram-Jones, K. Burke, R. J. Needs and C. A. Ullrich, *Phys. Rev. A: At., Mol., Opt. Phys.*, 2014, **90**, 042501.

78 B. Senjean, S. Knecht, H. J. A. Jensen and E. Fromager, *Phys. Rev. A: At., Mol., Opt. Phys.*, 2015, **92**, 012518.

79 B. Senjean, E. D. Hedegård, M. M. Alam, S. Knecht and E. Fromager, *Mol. Phys.*, 2016, **114**, 968.

80 J. C. Smith, A. Pribram-Jones and K. Burke, *Phys. Rev. B*, 2016, **93**, 245131.

81 B. Senjean and E. Fromager, *Phys. Rev. A*, 2018, **98**, 022513.

82 A. Nagy, *J. Phys. B: At., Mol. Opt. Phys.*, 1996, **29**, 389.

83 G. Paragi, I. K. Gyemnnt and V. E. VanDoren, *J. Mol. Struct.: THEOCHEM*, 2001, **571**, 153.

84 P.-F. Loos and P. M. W. Gill, *Wiley Interdiscip. Rev.: Comput. Mol. Sci.*, 2016, **6**, 410.

85 P.-F. Loos and P. M. W. Gill, *J. Chem. Phys.*, 2011, **135**, 214111.

86 P. M. W. Gill and P.-F. Loos, *Theor. Chem. Acc.*, 2012, **131**, 1069.

87 P.-F. Loos, *Phys. Rev. A: At., Mol., Opt. Phys.*, 2014, **89**, 052523.

88 P.-F. Loos, C. J. Ball and P. M. W. Gill, *J. Chem. Phys.*, 2014, **140**, 18A524.

89 P.-F. Loos, *J. Chem. Phys.*, 2017, **146**, 114108.

90 P.-F. Loos and E. Fromager, *J. Chem. Phys.*, 2020, **152**, 214101.

91 M. Levy, *Phys. Rev. A: At., Mol., Opt. Phys.*, 1995, **52**, R4313.

92 J. P. Perdew and M. Levy, *Phys. Rev. Lett.*, 1983, **51**, 1884.

93 E. Fromager, *Phys. Rev. Lett.*, 2020, in press, arXiv:2001.08605 [physics.chem-ph].

94 T. Gould and S. Pittalis, 2020, arXiv:2001.09429 [cond-mat.str-el].

95 T. Gould, *Approximately self-consistent ensemble density functional theory with all correlations*, 2020.

96 P. F. Loos, *QuAcK: a software for emerging quantum electronic structure methods*, 2019, https://github.com/pfloos/QuAcK.

97 T. H. Dunning Jr, *J. Chem. Phys.*, 1989, **90**, 1007.

98 R. A. Kendall, T. H. Dunning and R. J. Harisson, *J. Chem. Phys.*, 1992, **96**, 6796.

99 D. Woon and T. H. Dunning, *J. Chem. Phys.*, 1994, **100**, 2975.

100 R. Bast, *Numgrid: numerical integration grid for molecules*, 2020.

101 A. D. Becke, *J. Chem. Phys.*, 1988, **88**, 2547.

102 R. Lindh, P.-A. Malmqvist and L. Gagliardi, *Theor. Chem. Acc.*, 2001, **106**, 178.

103 A. T. B. Gilbert, N. A. Besley and P. M. W. Gill, *J. Phys. Chem. A*, 2008, **112**, 13164.

104 G. M. J. Barca, A. T. B. Gilbert and P. M. W. Gill, *J. Chem. Theory Comput.*, 2018, **14**, 1501.

105 G. M. J. Barca, A. T. B. Gilbert and P. M. W. Gill, *J. Chem. Theory Comput.*, 2018, **14**, 9.

106 P. A. M. Dirac, *Proc. Cambridge Philos. Soc.*, 1930, **26**, 376.

107 J. C. Slater, *Phys. Rev.*, 1981, **81**, 385.

108 C. Bottcher and K. Docken, *J. Phys. B: At. Mol. Phys.*, 1974, 7, L5.

109 E. Fromager, S. Knecht and H. J. Aa. Jensen, *J. Chem. Phys.*, 2013, **138**, 084101.

110 T. Stein, L. Kronik and R. Baer, *J. Am. Chem. Soc.*, 2009, **131**, 2818.

111 T. Stein, H. Eisenberg, L. Kronik and R. Baer, *Phys. Rev. Lett.*, 2010, **105**, 266802.

112 T. Stein, J. Autschbach, N. Govind, L. Kronik and R. Baer, *J. Phys. Chem. Lett.*, 2012, **3**, 3740.

113 S. Refaely-Abramson, S. Sharifzadeh, N. Govind, J. Autschbach, J. B. Neaton, R. Baer and L. Kronik, *Phys. Rev. X*, 2012, **109**, 226405.

114 S. H. Vosko, L. Wilk and M. Nusair, *Can. J. Phys.*, 1980, **58**, 1200.

115 P.-F. Loos and P. M. W. Gill, *Phys. Rev. A: At., Mol., Opt. Phys.*, 2009, **79**, 062517.

116 P.-F. Loos and P. M. W. Gill, *Phys. Rev. Lett.*, 2009, **103**, 123008.

117 P.-F. Loos and P. M. Gill, *Mol. Phys.*, 2010, **108**, 2527.

118 P.-F. Loos and P. M. W. Gill, *J. Chem. Phys.*, 2013, **138**, 164124.

119 J. Sun, J. P. Perdew, Z. Yang and H. Peng, *J. Chem. Phys.*, 2016, **144**, 191101.

120 J. Toulouse, A. Savin and H.-J. Flad, *Int. J. Quantum Chem.*, 2004, **100**, 1047.

121 Y. Garniron, K. Gasperich, T. Applencourt, A. Benali, A. Ferté, J. Paquier, B. Pradines, R. Assaraf, P. Reinhardt, J. Toulouse, P. Barbaresco, N. Renon, G. David, J. P. Malrieu, M. Véril, M. Caffarel, P. F. Loos, E. Giner and A. Scemama, *J. Chem. Theory Comput.*, 2019, **15**, 3591.

122 R. P. Madden and K. Codling, *Phys. Rev. Lett.*, 1963, **10**, 516.

123 A. Burgers, D. Wintgen and J.-M. Rost, *J. Phys. B: At., Mol. Opt. Phys.*, 1995, **28**, 3163.